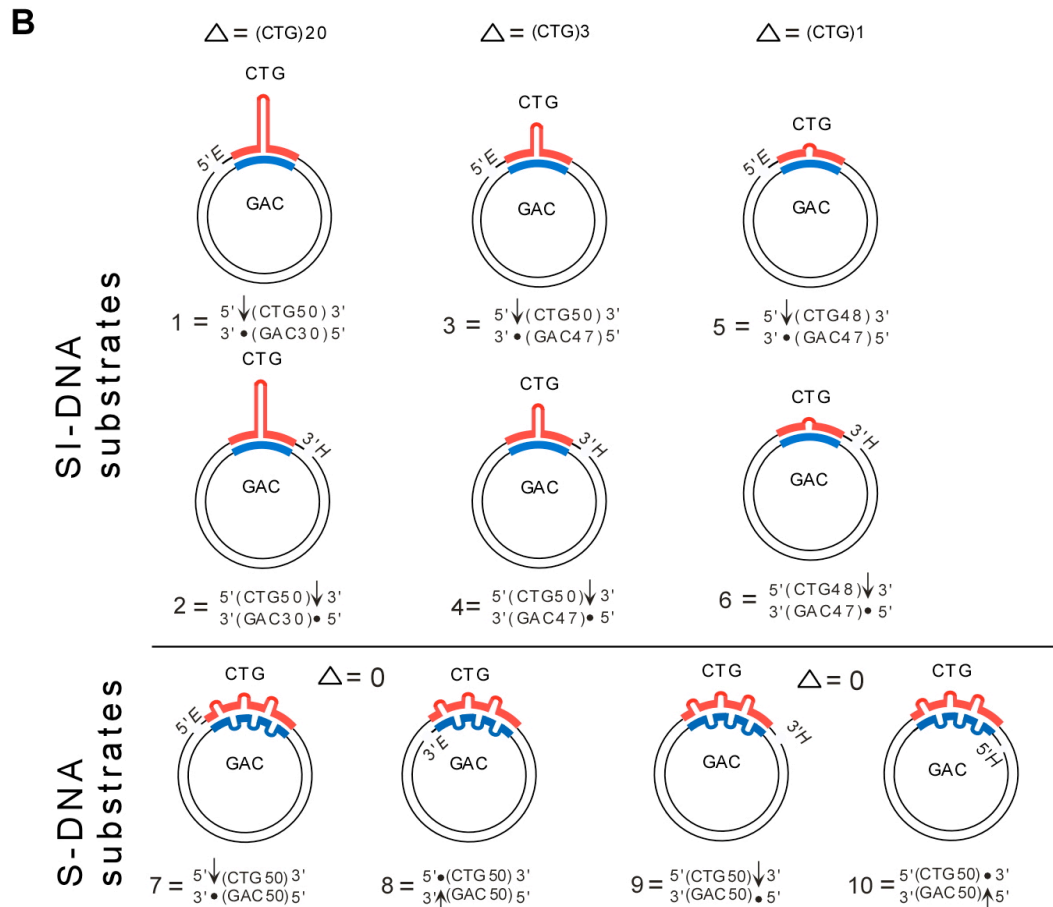
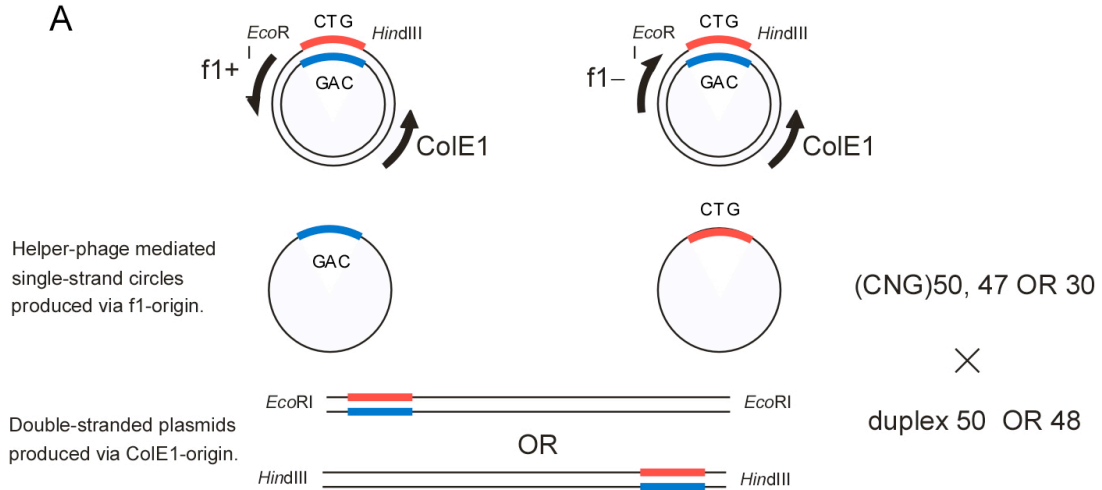


### Supplementary Figure Legends and Information

Isolated Short CTG/CAG DNA Slip-Outs are Efficiently Repaired by hMutS $\beta$ , Yet Clustered Slip-Outs Escape Repair.

Panigrahi GB et al.

Figure S1



### Figure S1 A: Preparation of circular slipped-heteroduplexes (SI-DNA and S-DNA).

Preparation of circular slipped-CTG/CAG hybrids has been outlined in detail<sup>1</sup>. Briefly, a set of double-stranded f1+ and f1- (CTG) $\bullet$ (CAG) clones containing 30, 47, 48 or 50 repeats enabled the production of circular single-stranded DNAs with (CAG) $n$  (f1+) or (CTG) $n$  (f1-) repeats, as well as duplex plasmids. Relative to the (CTG) $\bullet$ (CAG) tract this configuration of the f1 and ColE1 replication origins permitted stable propagation of the repeats in either single-stranded circular or duplex DNA preparations, respectively<sup>2</sup>. Circular ssDNAs were prepared from XL-1BlueMRF' cells transformed with the phagemid clones and infected with M13K07 helper phage. Circular ssDNAs were treated with RNaseA and DNaseI to eliminate contaminating RNA and dsDNAs, precipitated with PEG8000 and de-proteinised.

Ten circular slipped-hybrids were prepared by hybridising circular single-strand DNAs of one repeat length with linearised double-stranded plasmid DNAs of another repeat length. Heteroduplexing was performed as described<sup>1-5</sup> using a 1:5 molar ratio of single-stranded to double-stranded DNA and denatured in a solution of 0.5 M NaCl (yielding pH 13) and 500 mM NaOH at room temperature for 5 minutes. Samples were neutralised with a 50-fold volume of 50 mM Tris-HCl (pH 8), 5 mM EDTA, 0.2755 M NaCl, and renatured at 68°C for 3 hours, followed by two ethanol precipitations. Due to their unique electrophoretic mobility, circular slipped hybrids could be resolved and gel-purified from each of the starting reagents. All circular slipped hybrids co-migrated on 1% agarose (2 volts/cm) with nicked circular form II DNA, a form not present in any of the starting reagents and were gel-purified. Circular nicked preparations of S-DNA could not be purified from the fully-duplexed form, and hence harbored both slipped and fully-duplexed DNA.

### Figure S1 B: SI-DNA and S-DNA substrates used in the study

Schematic representation of circular hybrids with slipped (CTG) $x$  $\bullet$ (CAG) $y$  repeats SI-DNA (where  $x$  and  $y$  are 30, 47, 48, or 50 repeats, and  $x - y = 20, 3,$  or 1 repeat) and a unique nick at the *EcoRI* (*E*) or *HindIII* (*H*) site. The CAG and CTG tracts are colored blue and red, respectively. As indicated, nicks are located 5' or 3' of the slip-out, which is present in the nicked strand typical of predicted intermediates of expansion mutations. Substrate names identify the repeat lengths, sequences, strand polarity and nick location (arrow). Schematics of circular hybrids with homoduplex slipped (CTG) $50$  $\bullet$ (CAG) $50$  S-DNAs with a unique nick (5' or 3') located at an *HindIII* (*H*) site, co-purified with fully-duplexed forms.

1. Panigrahi GB et al. Slipped (CTG) $\bullet$ (CAG) repeats can be correctly repaired, escape repair or undergo error-prone repair. *Nat Struct Mol Biol* **12**, 654-62 (2005).
2. Iyer, R.R. & Wells, R.D. Expansion and deletion of triplet repeat sequences in *Escherichia coli* occur on the leading strand of DNA replication. *J Biol Chem* **274**, 3865-3877 (1999).
3. Pearson, C.E., Ewel, A., Acharya, S., Fishel, R.A. & Sinden, R.R. Human MSH2 binds to trinucleotide repeat DNA structures associated with neurodegenerative diseases. *Hum Mol Genet* **6**, 1117-1123. (1997).

4. Pearson, C.E. et al. Slipped-strand DNAs formed by long (CAG)•(CTG) repeats: slipped-out repeats and slip-out junctions. *Nucleic Acids Res* **30**, 4534-4547. (2002).
5. Tam, M. et al. Slipped (CTG)•(CAG) repeats of the myotonic dystrophy locus: surface probing with anti-DNA antibodies. *J Mol Biol* **332**, 585-600. (2003).

Figure S2

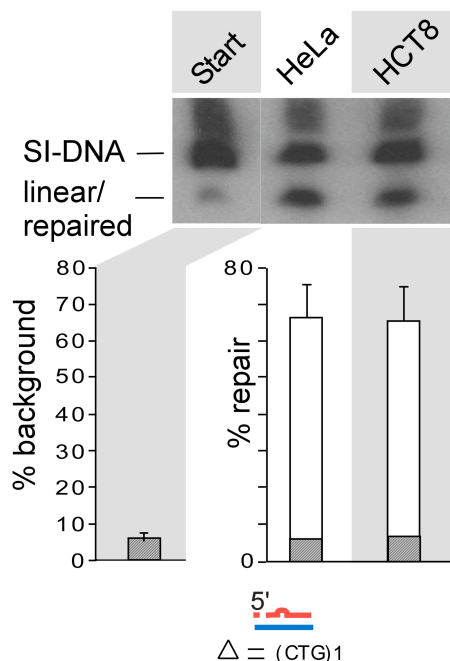


**Figure S2: Repair by hMSH6-deficient HCT8 cell extracts**

Repair of short slip-outs does not require hMSH6. Repair assays in 50  $\mu\text{L}$  reaction volumes, 22 fmol of substrate, were incubated with 90  $\mu\text{g}$  cell extracts for 30 minutes. Efficiencies were calculated on a molar level by densitometric analysis of Southern blots. Starting material is on the left. A graphical representation of 3 replicates shows the starting background (hatched bars) and repair (white bars).

**Figure S3: MMR protein levels in cell extracts: Simultaneous Western Blotting**

#### Methods: Simultaneous Western Blot of MMR Proteins

Here we present some points for this novel protocol, which will be outlined in detail elsewhere. Cell extracts were sonicated (Misonix Sonicator 3000) and protein concentration was determined using the Bradford Reagent (Bio-Rad). A total of 50  $\mu\text{g}$  of each sample was diluted in 4xLaemmli loading buffer and boiled for 5 minutes at 95°C. Samples were separated on an 8% SDS-PAGE gel alongside Pageruler™ prestained protein ladder (Fermentas cat. #SM0671). Electrophoresis permitted excellent separation of each of proteins hMSH6 (160 kDa), hMSH3 (127 kDa), hMSH2 (100 kDa), and actin (43 kDa). The SDS-PAGE gels were transferred to a polyvinylidene fluoride membrane (PVDF) (Roche) and membranes were blocked for a minimum of 30 minutes in 5% Casein solution (5% w/v casein milk powder; 1X Phosphate-buffered saline pH 7.4, 0.1% Tween-20 (1XPBS-T). Membranes were simultaneously incubated for 2 days at 4°C in primary antibodies, which were previously titrated to equivalent intensities of anti-MSH3 antibody (1/100, BD Biosciences cat. #611390), anti-MSH2 (1/2500, Calbiochem cat. #NA26), anti-MSH6 (1/1500, BD Biosciences cat. #610919) and anti-actin (1/15000, BD Biosciences cat. #612656). This will be described elsewhere. Membranes were washed 3 x 10

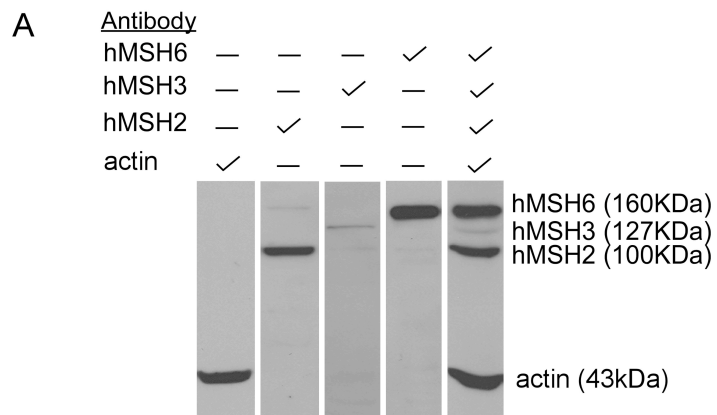
minutes in 1X PBS-T and probed with anti-mouse, HRP-conjugated secondary antibody (GE Healthcare cat. #NA931). Chemiluminescence was captured on Hyblot CL (Denville Scientific) using Amersham™ ECL™ Western Blotting Detection Reagent (GE Healthcare). Hyblot CL film was developed using the Kodak X-OMAT 2000A processor.

Assessments are made from a single gel, a single blot, a single probing with multiple primary antibodies, a single probing with the secondary antibody, and a single film exposure. There are several advantages to simultaneously measuring multiple proteins in a single sample compared to independent measurement of each protein alone in an individual sample. Other methods commonly used to quantitate multiple proteins in a sample such as replica blots or sequential probing and sequential stripping of one membrane with different antibodies suffer deleterious steps to equal loading and transfer of proteins or protein degradation - which can hamper quantitative comparison of proteins. Simultaneous blotting eliminates variability resulting from sample handling prior to electrophoresis (e.g., variability in sample isolation, dilution, pipetting, or loading errors). Simultaneous blotting eliminates errors of various film exposure times, permitting direct comparison of all protein levels. Simultaneous analysis of multiple proteins in a sample provides an internal standard, which allows the values obtained to be normalized. In Figure 2A and Figure S2B this last advantage is illustrated by comparing the relative levels of hMSH2 to actin, which shows limited variation, allowing for a rapid comparison of the levels of hMSH3 to hMSH6 between different cell extracts.

**Figure S3A: Probing with individual versus simultaneous antibodies:**

To ensure that there was no cross-reactivity the following experiment was performed. HeLa cell extracts (50 µg) were loaded into 5 consecutive lanes, and proteins electrophoretically resolved on denaturing SDS PAGE and transferred to PVDF membrane.

Each of the first four lanes was independently probed using a single primary antibody to either hMSH6, hMSH3, hMSH2, or actin. The fifth lane was simultaneously probed using all four antibodies. Blotting using the individual antibodies (to either hMSH6, hMSH3, hMSH2, or actin) yielded essentially only the individual bands, with the exception of hMSH2 and hMSH6, which in some extract preparations occasionally yielded additional faster migrating bands, presumably degradation products. The background staining caused by the four antibodies was moderate. Importantly, the background staining caused by any of these antibodies did not appear within regions of the blot where the proteins recognized by the other three antibodies were located.



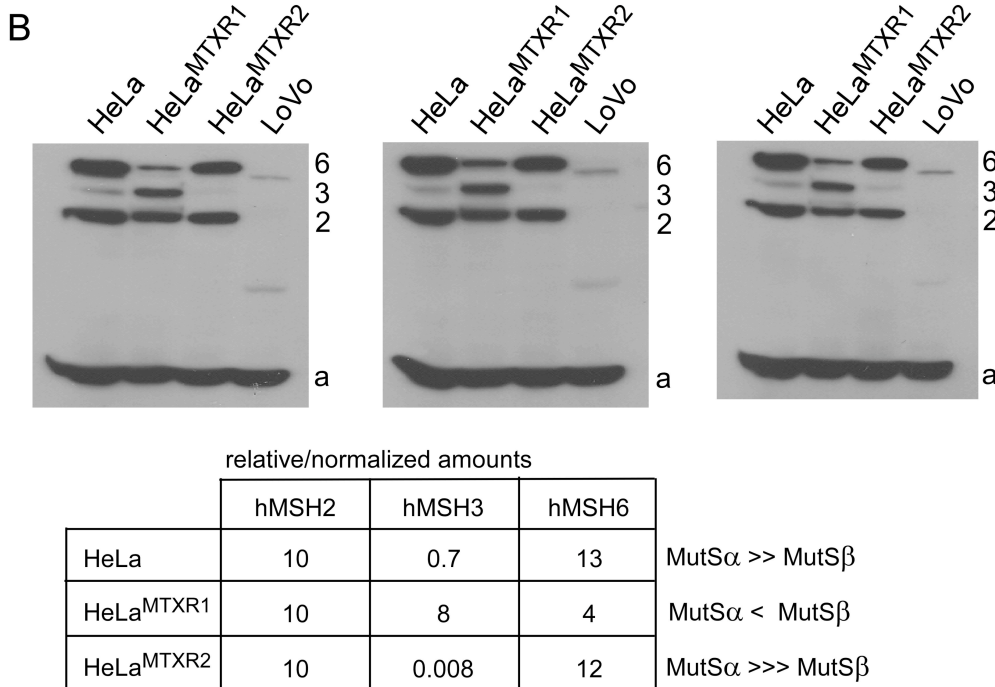


**Figure S3B: Simultaneous Blotting of MMR proteins in cell extracts is reproducible**

Extracts (50  $\mu$ g) from HeLa, HeLa<sup>MTXR1</sup>, HeLa<sup>MTXR2</sup>, and LoVo cells were loaded into 4 consecutive lanes on 3 separate gels, blotted and simultaneously probed with antibodies to hMSH3, hMSH2, hMSH6, and actin, as described above. All membranes were simultaneously exposed to film for the same time. Densitometric analysis of the relative intensities of bands for hMSH2, hMSH3, hMSH6 relative to actin within an extract reveal the relative amounts these proteins in the sample (table). Our relative amounts of hMSH3 to hMSH6 is similar to other reports where hMSH6 protein is present at 4-12 times the amount of hMSH3, and the sum of hMSH3 and hMSH6 proteins is approximately equal to the amount of hMSH2 protein (1).

1. Chang DK, et al. (2000) Steady-state regulation of the human DNA mismatch repair system. *J Biol Chem* 275:29178.

Figure S4

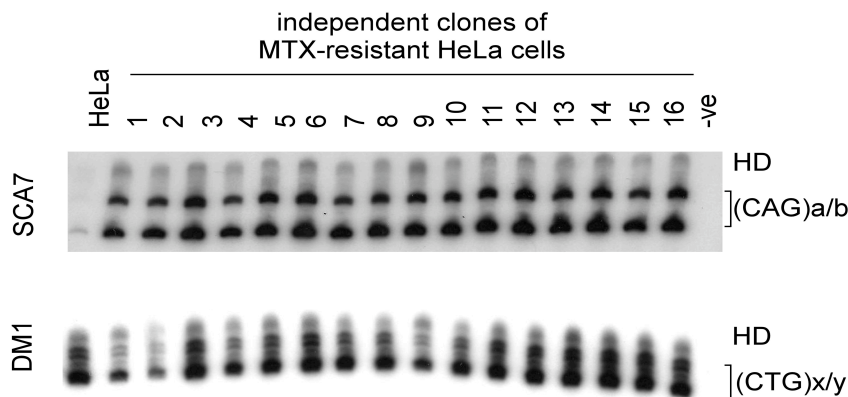


**Figure S4: hMSH3 levels do not affect stability of short endogenous CTG/CAG loci.**

We assessed the possible altered instability at endogenous trinucleotide repeats by the overexpression of

hMSH3 in the DHFR amplified methotrexate HeLa cell derivatives. We assessed the DM1 and spinocerebellar ataxia type 7 loci, two disease loci that display the highest levels of trinucleotide repeat instability (2, 3). HD indicates PCR heteroduplexes. Primers and PCR amplification conditions have been described (4, 5). None of the clones displayed any alterations of repeat lengths at these loci (Fig. S3). It is noteworthy that the repeat tract lengths at the HeLa endogenous loci are shorter (DM1 x/y = 11/14 repeats; SCA7 a/b repeats) than the typical lengths that display instability (>35 to as many as 6,550 repeats). Previous reports did not observe enhanced instability of short tract lengths at various disease-associated trinucleotide repeats in MMR-deficient cell lines including HCT116 which is genetically deficient for hMSH3 (6). This reveals that overexpression of hMSH3 does not lead to increased instability of shorter than threshold length CTG/CAG tracts at disease loci. This might suggest that the effect of hMSH3 protein levels upon trinucleotide repeat instability may be tract length dependent.

1. Rüschoff J, et al. (1998) Aspirin suppresses the mutator phenotype associated with hereditary nonpolyposis colorectal cancer by genetic selection. *Proc Natl Acad Sci U S A* 95:11301-11306.
2. Pearson CE, et al. (2005) Repeat instability: mechanisms of dynamic mutations. *Nat Rev Genet* 6:729-742.
3. Cleary JD, Pearson CE (2003) The contribution of *cis*-elements to disease-associated repeat instability: Clinical and experimental evidence. *Cytogenet & Genome Res* 100:25-55.
4. Yang Z, Lau R, Marcadier JL, Chitayat D, Pearson CE (2003) Replication inhibitors modulate instability of an expanded trinucleotide repeat at the myotonic dystrophy type 1 disease locus in human cells. *Am J Hum Genet* 73:1092-1105.
5. Libby RT, et al. (2008) CTCF cis-regulates trinucleotide repeat instability in an epigenetic manner: a novel basis for mutational hot spot determination. *PLoS Genet* 4:e1000257.
6. Kramer PR, Pearson CE, Sinden RR (1996) Stability of triplet repeats of myotonic dystrophy and fragile X loci in human mutator mismatch repair cell lines. *Hum Genet* 98:151-157.

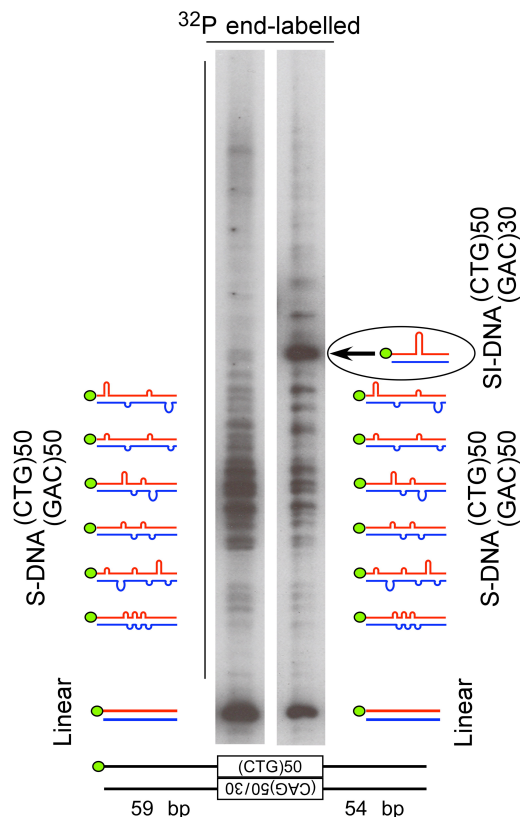


**Figure S5: Multiple slip-outs in S-DNAs versus an isolated slip-out in SI-DNAs**

Structural analysis by high-resolution polyacrylamide gel electrophoresis of uniquely radiolabeled (dot) DNA fragments containing homoduplex slipped (CTG)<sub>50</sub>•(CAG)<sub>50</sub> S-DNAs with fully-duplexed form (left lane) and mixtures of this with heteroduplex slipped (CTG)<sub>50</sub>•(CAG)<sub>30</sub> SI-DNA (right lane, arrow). Schematics depict the multiple short slip-outs in S-DNAs and the unique slip-out in SI-DNA. Autorad is a single gel and the same exposure time, intervening lanes have been excised for presentation. For details see Figure 2 in (1 and (2-7). Unlike these linear preparations, circular substrates of SI-DNA contain only the heteroduplex, while S-DNA preparations also contain fully-duplexed forms.

1. Pearson CE, Ewel A, Acharya S, Fishel RA, & Sinden RR (1997) Human MSH2 binds to trinucleotide repeat NA structures associated with neurodegenerative diseases. *Hum Mol Genet* 6:1117-1123
2. Pearson CE, et al. (2002) Slipped-strand DNAs formed by long (CAG)•(CTG) repeats: slipped-out repeats and slip-out junctions. *Nucleic Acids Res* 30:4534-4547.
3. Pearson CE, et al. (1998) Interruptions in the triplet repeats of SCA1 and FRAXA reduce the propensity and complexity of slipped strand DNA (S-DNA) formation. *Biochemistry* 37:2701-2708.
4. Pearson CE, Wang YH, Griffith JD, & Sinden RR (1998) Structural analysis of slipped-strand DNA (S-DNA) formed in (CTG)<sub>n</sub>.(CAG)<sub>n</sub> repeats from the myotonic dystrophy locus. *Nucleic Acids Res* 26:816-823.
5. Tam M, et al. (2003) Slipped (CTG)•(CAG) repeats of the myotonic dystrophy locus: surface probing with anti-DNA antibodies. *J Mol Biol* 332:585-600.
6. López Castel A, Tomkinson AE, Pearson CE (2009) CTG/CAG repeat instability is modulated by the levels of human DNA ligase I and its interaction with proliferating cell nuclear antigen: a distinction between replication and slipped-DNA repair. *J Biol Chem* 284:26631-26645.
7. Panigrahi GB, Lau R, Montgomery SE, Leonard MR, Pearson CE (2005) Slipped (CTG)•(CAG) repeats can be correctly repaired, escape repair or undergo error-prone repair. *Nat Struct Mol Biol* 12:635-637.

**Figure S6: Multiple slip-outs interfere with repair, regardless of nick location.**

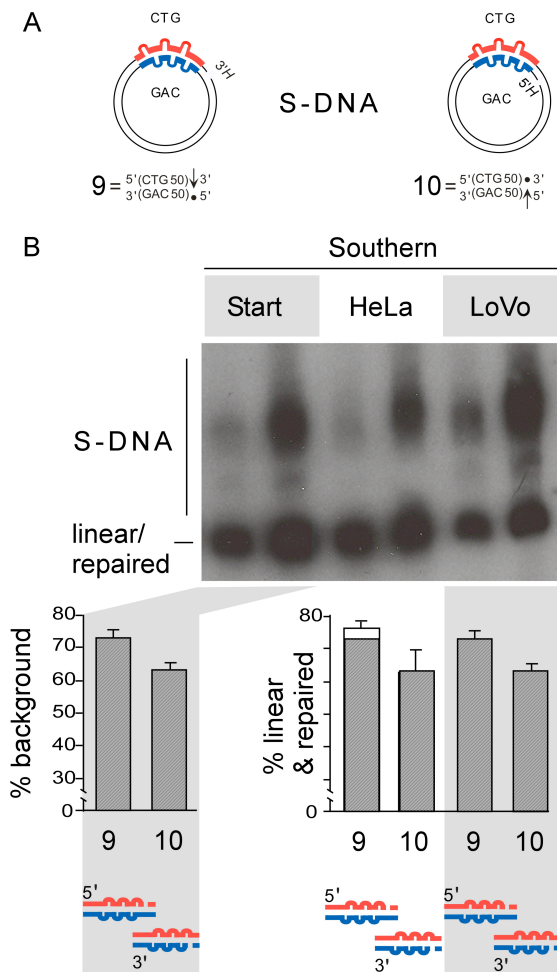


**Figure S6A:**

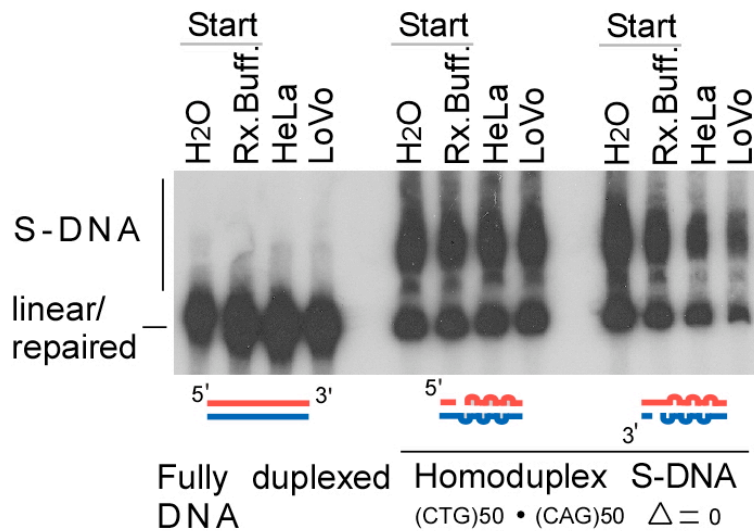
Schematics of circular hybrids with homoduplex slipped (CTG)<sub>50</sub>•(CAG)<sub>50</sub> S-DNAs with a unique nick (5' or 3') located at an *Hind*III (H) site, co-purified with fully-duplexed forms.

**Figure S6B:**

A representative Southern blot analysis of repair products. Repair efficiencies including starting fully-duplexed linear non-slipped material for the S-DNA substrates using MMR-proficient (HeLa) and MMR-deficient (LoVo) cell extracts, with the starting material shown on the left. Efficiencies calculated for three replicates. Starting material is on the left. A graphical representation of 3-6 replicates shows the starting background (hatched bars) and repair (white bars). See also Fig. 3 where nicks (5' or 3') were located upstream of the repeat at an *Eco*RI (E) site.

### Figure S7 : Lack of interconversion between S-DNA and fully-duplexed DNA

Slipped-DNA structures exhibit remarkable biophysical stability as previously demonstrated by: **1)** their shifted out-of-register mispairing is independent of supercoiling – they are stable in linear DNA; **2)** the absence of interconversion of purified slipped-DNA to fully duplexed linear from or to other slipped isoforms, or of linear form to slipped-DNAs, even following extended incubation under elevated temperatures of 37 °C - 55 °C<sup>1</sup>, **3)** We also demonstrated that



interconversions could not be forced by phenol extraction with strong vortexing<sup>1</sup>, which is known to accelerate the reassociation of DNA<sup>2</sup>.

To determine if such interconversions occurred under our repair reaction conditions (fully-duplexed to S-DNAs or S-DNAs to fully-duplexed forms) we performed the following experiment (see figure above). Circular DNAs with (CTG)50•(CAG)50 repeats either in the fully-duplexed form, or slipped S-DNA forms with 5' or

3' nicks were either mock repaired (reaction buffer) without added protein, or were treated/repaired by HeLa or LoVo cell extracts. Each reaction was compared to the starting DNA in water. (Circular nicked preparations of S-DNA could not be purified from the fully-duplexed form, and hence harbored both slipped and fully-duplexed DNA.) There was no interconversion of the fully-duplexed repeats to slipped S-DNAs under repair reaction conditions with or without protein (first four lanes). Thus the limited amount of repair that does occur for S-DNAs to become fully-duplexed does not then get converted back to S-DNA. There was no interconversion of the slipped S-DNAs to fully-duplexed form as evidenced by the similar proportion of each following treatment. While we were unable to purify circular hybrids from each other, previously published experiments using purified linear S-DNAs did not show any interconversion<sup>1</sup>. Thus, the poor repair S-DNAs is an appropriate interpretation, and excludes the alternative interpretation that repair is occurring but the repair products (as fully-duplexed forms) are converting back to S-DNA form.

1. Pearson CE & Sinden RR, 1996, Alternative structures in duplex DNA formed within the trinucleotide repeats of the myotonic dystrophy and fragile X loci, *Biochemistry*, **35**:5041-53.

2. Kohne DE et al., 1977, Room temperature method for increasing the rate of DNA reassociation by many thousandfold: the phenol emulsion reassociation technique, *Biochemistry*, **16**:5329-41.



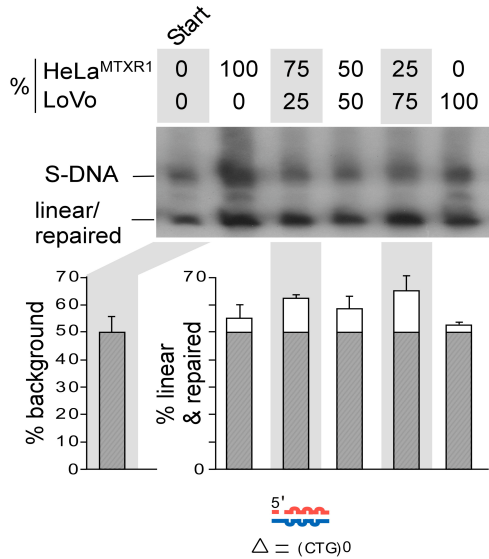


**Figure S8: Multiple slip-outs interfere with repair at various MutS $\beta$  concentrations**

MutS $\beta$  concentration-sensitive short CTG slip-out repair. A homoduplex slipped (CTG)<sub>50</sub>•(CAG)<sub>50</sub> S-DNA substrate was processed with mixtures of the hMSH3 overexpressed (HeLa<sup>MTXR1</sup>) and LoVo (MMR-deficient) cell extracts to dilute hMSH3 levels. Representative Southern blot is shown, with starting material on the left. A graphical representation of 3-6 replicates shows the starting background (hatched bars) and repair (white bars).

**Figure S9**

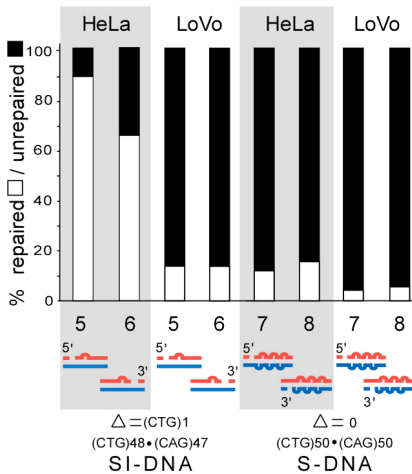


**Figure S9: Corrected and normalized repair efficiencies for the single (CTG)<sub>1</sub> slip-out SI-DNA (from Fig.1A) and homoduplex slipped S-DNAs (from Fig. 3).** Correction removes portion of fully-duplexed linear non-slipped material present in S-DNA and SI-DNA preparations prior to repair; this correction reveals the portion that escaped repair (filled) and the portion that was repaired (hollow).

## Methods:

### Repair Reactions:

Slipped-strand and G-T repair reactions (50  $\mu$ l) were performed as described<sup>1,2</sup>. Briefly, 50 ng of slipped substrate was incubated in 15 mM sodium phosphate, 100  $\mu$ g/ml creatine kinase, 40 mM creatine phosphate, 4 mM ATP, 200  $\mu$ M each CTP, GTP and UTP, 33  $\mu$ M each dATP, dGTP, P-

dCTP and dTTP and 15  $\mu$ l of cell extracts (6  $\mu$ g protein/ $\mu$ l) at 37°C for 30 minutes. An equal volume of stop solution (2 mg/ml proteinase K, 2% SDS and 50 mM EDTA (pH 8.0)) was added and incubated at 37°C for 30 minutes after which 15  $\mu$ g of tRNA was added to each reaction, and proteins extracted with phenol/chloroform, ethanol precipitated and resuspended in water. The repeat containing fragment was liberated by *EcoRI/HindIII* digestion and analysed on a 4% native polyacrylamide gel.

### Repair efficiencies

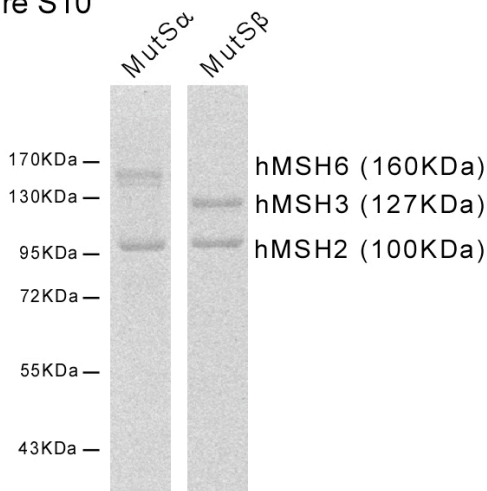
Repair efficiencies were determined on a molar level by Southern blot probing of reaction products, as described<sup>1,2</sup>. Following release of the repeat-containing fragment (*EcoRI/HindIII*) and resolution on native acrylamide, products were electrotransferred to membrane and hybridized to a radiolabelled *EcoRI/HindIII* fragment containing only 17 repeats. Repair efficiency is the proportion of radio-intensity of the repeat-containing product relative to all repeat-containing fragments (ImageQuant Molecular Dynamics v1.2). The same analysis was performed for base-base repair reactions. All starting un-processed substrates were assessed simultaneously. G-T mismatch repair efficiencies were assessed identically. Quantifications are the average of 3-6 independent experiments. Non-specific repair was assessed by incorporation of radionucleotides, as published<sup>1,2</sup>.

1. Panigrahi GB et al., Slipped (CTG) $\cdot$ (CAG) repeats can be correctly repaired, escape repair or undergo error-prone repair. *Nat Struct Mol Biol* **12**, 654-62 (2005).
2. López Castel A et al., CTG/CAG repeat instability is modulated by the levels of human DNA ligase I and its interaction with proliferating cell nuclear antigen: a distinction between replication and slipped-DNA repair. *J Biol Chem* **284**:26631-26645 (2009).

### Purification of hMutS $\alpha$ and hMutS $\beta$

Baculoviruses for expressing his-tagged hMSH2, hMSH3, and hMSH6 were kindly provided by Guo-Min Li. Expression and purification to near homogeneity were as we previously outlined (1) with modifications (2-4). Recombinant human hMutS $\alpha$  and hMutS $\beta$  were expressed in insect

Figure S10



cells and purified to near homogeneity. High Five cells were grown to a density of  $2 \times 10^6$  cells/mL and infected simultaneously with his-hMSH3 and his-hMSH2 viruses or his-hMSH6 and his-hMSH2 viruses. Infected cells were pelleted and resuspended in 25 mM HEPES pH 8.1, 300 mM NaCl, 20 mM imidazole, 10% glycerol and protease inhibitors (Calbiochem protease inhibitor cocktail set VII). Cells were lysed by sonication and centrifuged (125,000  $\times$ g, 1 hour). Supernatant was applied to a HisTrap HP column (GE Healthcare), and eluted with a linear gradient of 20 mM to 200 mM imidazole. Fractions enriched for the proteins were pooled and applied to a HiTrap heparin HP column (GE Healthcare), then eluted in a linear gradient from 300 mM to 1M

NaCl in 25 mM HEPES pH 8.1, 1 mM DTT, 0.1 mM EDTA, 10% glycerol. Enriched fractions were diluted to 100 mM NaCl, applied to a HiTrap Q FF column (GE Healthcare), then eluted from 100 mM to 1 M NaCl. Fractions containing MutS $\alpha$  or MutS $\beta$  were dialyzed against 25 mM HEPES pH 8.1, 100 mM NaCl, 1 mM DTT, 0.1 mM EDTA, 20% glycerol.

1. Pearson CE, Ewel A, Acharya S, Fishel RA, Sinden RR (1997) Human MSH2 binds to trinucleotide repeat DNA structures associated with neurodegenerative diseases. *Hum Mol Genet* 6:1117-1123.
2. Wilson T, Guerrette S, Fishel R (1999) Dissociation of mismatch recognition and ATPase activity by hMSH2-hMSH3. *J Biol Chem* 274:21659-21664.
3. Zhang Y, et al. (2005) Reconstitution of 5'-directed human mismatch repair in a purified system. *Cell* 122:693-705.
4. Tian L, et al. (2009) Mismatch recognition protein MutSbeta does not hijack (CAG)n hairpin repair *in vitro*. *J Biol Chem* 284:20452-20456.